The endocochlear potential depends on two K^+ diffusion potentials and an electrical barrier in the stria vascularis of the inner ear

Fumiaki Nin*†, Hiroshi Hibino*, Katsumi Doi‡, Toshihiro Suzuki†, Yasuo Hisa†, and Yoshihisa Kurachi*§

*Division of Molecular and Cellular Pharmacology, Department of Pharmacology, and ‡Department of Otolaryngology, Graduate School of Medicine, Osaka University, 2-2 Yamada-oka, Suita, Osaka 565-0871, Japan; and †Department of Otolaryngology–Head and Neck Surgery, Kyoto Prefectural University of Medicine, Kyoto 602-8566, Japan

Communicated by A. James Hudspeth, The Rockefeller University, New York, NY, December 6, 2007 (received for review October 24, 2007)

An endocochlear potential (EP) of +80 mV is essential for audition. Although the regulation of K^+ concentration ($[K^+]$) in various compartments of the cochlear stria vascularis seems crucial for the formation of the EP, the mechanism remains uncertain. We have used multibarreled electrodes to measure the potential, $[K^+]$, and input resistance in each compartment of the stria vascularis. The stria faces two fluids, perilymph and endolymph, and contains an extracelluar compartment, the intrastrial space (IS), surrounded by two epithelial layers, the marginal cell (MC) layer and that composed of intermediate and basal cells. Fluid in the IS exhibits a low $[K^+]$ and a positive potential, called the intrastrial potential (ISP). We found that the input resistance of the IS was high, indicating this space is electrically isolated from the neighboring extracellular fluids. This arrangement is indispensable for maintaining positive ISP. Inhibiting the K^+ transporters of the stria by anoxia, ouabain, or bumetanide caused the $[K^+]$ of the IS to increase and the intracellular $[K^+]$ of MCs to decrease, reducing both the ISP and the EP. Calculations indicate that the ISP represents the K^+ diffusion potential across the apical membranes of intermediate cells through Ba^{2+}-sensitive K^+ channels. The K^+ diffusion potential across the apical membranes of MCs also contributes to the EP. Because the EP depends on two K^+ diffusion potentials and an electrical barrier in the stria vascularis, interference with any of these elements can interrupt hearing.

hearing | ion transport | potassium

The cochlea of the inner ear is filled with two extracellular fluids, perilymph and endolymph. Endolymph contains ≈150 mM K^+, 2 mM Na^+, and 20 μM Ca^{2+} and exhibits a potential of +80 mV, the endocochlear potential (EP), relative to either blood plasma or perilymph (1). Hair cells, the receptors for hearing, lie above the basilar membrane with their apical surfaces exposed to endolymph and their basolateral surfaces to perilymph. Vibration of the basilar membrane opens mechanosensitive channels in hair-cell stereocilia; the ensuing K^+ influx from endolymph excites the cells (2). The EP enhances the sensitivity of hair cells by increasing the driving force not only for K^+ influx but also for the permeation of Ca^{2+} that amplifies the motility of hair bundles (3, 4).

After exiting hair cells on their basolateral surfaces, K^+ must cycle back to the endolymph through a pathway comprising perilymph, supporting cells, the spiral ligament, and the stria vascularis (5–7) (Fig. 1*A*). The stria vascularis consists of inner and outer epithelial layers. The narrow extracellular space of 15 nm separating the two layers, the intrastrial space (IS), widens to contain numerous capillaries (8). The inner epithelial layer is composed of marginal cells (MCs) whose apical membranes face endolymph. The outer layer consists of intermediate cells (ICs) and basal cells (BCs) that are apposed to fibrocytes of the spiral ligament (8) (Fig. 1*B*). The ICs, BCs, and fibrocytes are extensively connected through gap junctions and thus form an electrical syncytium (9, 10). Tight junctions between cells in the inner and outer layers and those in the vascular endothelial cells provide boundaries between the IS and endolymph, perilymph, and blood (11).

Several K^+ channels and transporters occur in various compartments of the stria vasularis and have been shown to be involved in EP formation (Fig. 1*B*). Na^+,K^+-ATPase and Na^+,K^+,$2Cl^-$-cotransporter (NKCC) are localized on the basolateral membranes of MCs (12, 13). Inhibition of either transporter suppresses the EP (14), and genetic disruption of NKCC causes hearing loss (15–17). Two types of K^+ channels are expressed in the stria vascularis. The inwardly rectifying channel Kir4.1 occurs in the apical membranes of ICs (18, 19); inhibition or knockout strongly reduces the EP (20–22). Another K^+ channel, KCNQ1/KCNE1, occurs in the apical membranes of MCs. Mice lacking this channel are deaf because of the collapse of the endolymphatic space (23–25).

The fluid in the IS has a low $[K^+]$ but a positive potential similar to the EP (26, 27). It has been hypothesized that the intrastrial potential (ISP) is the origin of the EP (26). The low $[K^+]$ in the IS fluid is thought to be maintained by K^+ transporters located in the basolateral membranes of MCs. An electrophysiological study of isolated ICs suggested that the ISP is generated by K^+ diffusion across the apical membranes of ICs through Kir4.1 channels (28). Although inhibition of the Na^+,K^+-ATPase reduced the EP to −10 mV, the inside of the stria vascularis still exhibited a potential of +14 mV (29). This result implies that the ISP is not exclusively responsible for formation of the EP. Because of technical difficulties, however, no extensive studies have been performed *in vivo* to clarify the relationship between the ISP and the EP, and the machinery underlying the formation of ISP and EP has not been established.

In this study, we simultaneously measured the electrical potential, $[K^+]$, and input resistance in each compartment of the lateral cochlear wall under various conditions. We have not only verified the hypothesis for formation of the ISP *in vivo* but have also identified other essential elements determining the EP.

Results

Measurement of Potential, $[K^+]$, and Resistance of Microcompartments in the Lateral Cochlear Wall. The passage of a double-barreled, K^+-selective electrode from the perilymph to the IS elicited a stereotyped sequence of events (Fig. 2*A*). At the outset,

Author contributions: F.N. and H.H. contributed equally to this work; H.H. and Y.K. designed research; F.N., H.H., and K.D. performed research; T.S. and Y.H. contributed new reagents/analytic tools; F.N. and H.H. analyzed data; and F.N., H.H., and Y.K. wrote the paper.

The authors declare no conflict of interest.

§To whom correspondence should be addressed. E-mail: ykurachi@pharma2.med.osaka-u.ac.jp.

This article contains supporting information online at www.pnas.org/cgi/content/full/0711463105/DC1.

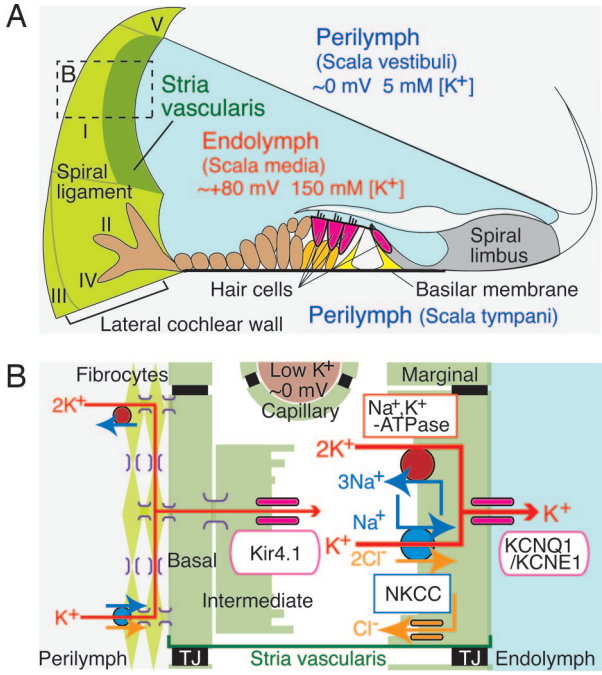

Fig. 1. Structure of the cochlea and its lateral wall. (*A*) The ionic composition and potential of the endolymph are maintained by the cells in the lateral wall of the cochlea (on the left). The locations of five types of fibrocytes are indicated by roman numerals. (*B*) A schematic enlargement of the boxed region in *A* depicts the ion-transport mechanisms involved in the formation of the EP. TJ, tight junction.

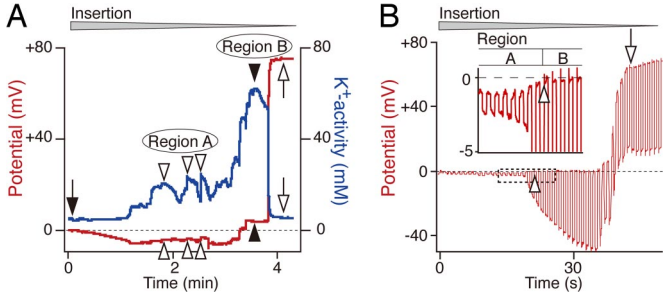

Fig. 2. Electrochemical properties of compartments in the lateral cochlear wall. (*A*) A recording of the potential (red) and aK^+ (blue) with a double-barreled K^+-selective electrode driven through the lateral wall commences with the electrode in perilymph (filled arrow). Open and filled arrowheads, respectively, point to the two regions that exhibit different profiles. After encountering the distinct profiles of Regions A and B, the electrode reached the IS (open arrows). In this and subsequent recordings, the wedge above the trace indicates the period during which the electrode was advanced. (*B*) A single-barreled electrode made simultaneous measurements of the potential and input resistance in the lateral wall. The electrode was driven through the lateral wall while being stimulated by constant current pulses (25-nA/pulse, duration 400 msec). At the point where the potential became slightly positive (open arrowheads), the input resistance increased greatly; this combination signaled entry from perilymph in Region A into the inside of the syncytium, Region B. Boxed area is enlarged in *Inset*. Further insertion of the electrode resulted in detection of the regions showing highly positive potential with high input resistance (open arrow), which might represent the feature of the IS fluid or MCs.

the electrode in perilymph recorded a K^+ activity (aK^+) of 4 mM (26, 27). On further insertion but before encountering the IS, we identified two regions showing characteristic alterations in aK^+ and potential. The first, Region A, exhibited a moderately elevated aK^+ of 20–24 mM with a slightly negative potential of −4 to −5 mV. The second, Region B, showed a greater aK^+ of ≈60 mM and a slightly positive potential of ≈+3 mV. When the electrode was further advanced, the potential abruptly became highly positive (+75 mV), and the aK^+ dropped to 5 mM, indicating that the electrode had entered the IS (26, 27). Regions A and B could in some instances be measured repeatedly during a single insertion of the electrode, whereas each of them appeared only once in other cases. In nine animals, we detected Region A six times (aK^+ = 19.0 ± 7.1 mM, range 6.1–26.1 mM; potential, −3.8 ± 1.8 mV, range −1.0 to −6.5 mV), and Region B eight times [aK^+ = 62.0 ± 8.7 mM, range 45.3–72.8 mM; potential, +2.0 ± 1.4 mV, range + 0.2 mV to + 3.8 mV; supporting information (SI) Fig. 7].

To identify the compartments of the stria vascularis corresponding to Regions A and B, we used a bridge-balance amplifier to record the input resistance and potential with a single-barreled electrode. In Region A with a potential of −1 mV, the input resistance was low (200 kΩ; Fig. 2*B*), implying that the electrode was located in perilymph. With further insertion of the electrode, the potential remained slightly positive at +0.2 mV, but the input resistance gradually increased to 2 MΩ, indicating that the electrode had entered Region B (Fig. 2*B*). Because the increased resistance indicated that the electrode had reached a restricted compartment surrounded by the cell membrane, Region B may represent the intracellular portion of the syncytium composed of fibrocytes, ICs, and BCs. When we advanced the electrode still further, the potential abruptly became very positive (+75 mV), whereas the input resistance remained at 2.4 MΩ (Fig. 2*B*): the electrode might have entered either the IS or the MCs. Similar results were obtained in six independent experiments.

The fingerprints of the IS are a highly positive potential (the ISP) and a low [K^+] (26, 27). The results above suggest that high-input resistance is another feature of the IS. To test this, we simultaneously recorded the potential, aK^+, and input resistance with a double-barreled electrode (Fig. 3). In this experiment, the electrode passed from the perilymph through the syncytium and then reached the IS (potential, +64 mV; aK^+, 3 mM). The input resistance, which was only 100 kΩ in the perilymph, increased to 300 kΩ in the cellular syncytium of Region B and finally reached 2.0 MΩ in the IS. Anoxia applied during recording at the final site elevated aK^+ and markedly suppressed the potential, confirming that the region was the IS (see also Fig. 4). Both the potential and the aK^+ recovered upon return to normoxia. When the electrode was advanced farther, the input resistance rapidly diminished, and aK^+ markedly increased, indicating that the electrode had entered the endolymph. In this recording, we could not detect the feature of MCs [high aK^+ (but <100 mM) and high potential; see Fig. 5]. It might be mainly due to the following difficulty. The MC monolayer is thin, and the double-barreled electrode is relatively thick. Thus, the electrode, when promptly inserted from the IS to the endolymph, as in the case of Fig. 3, could sometimes reach the endolymph apparently without recording the potential and aK^+ of MCs. Upon withdrawal of the electrode to the perilymph, the potential, aK^+, and input resistance all returned to their initial levels. We observed the same results in three trials. A high resistance therefore separates the fluid in the IS from the neighboring extracellular fluids, i.e., the perilymph, endolymph, and blood. This resistance isolates the IS electrically and thus permits the formation of its highly positive ISP.

Effects of Inhibiting Strial K^+ Transport on the Potential and aK^+. To test the hypothesis for the formation of the EP and ISP (26), we simultaneously monitored these two potentials and aK^+ of the IS fluid (aK^+_{IS}) during inhibition of the strial K^+-transport

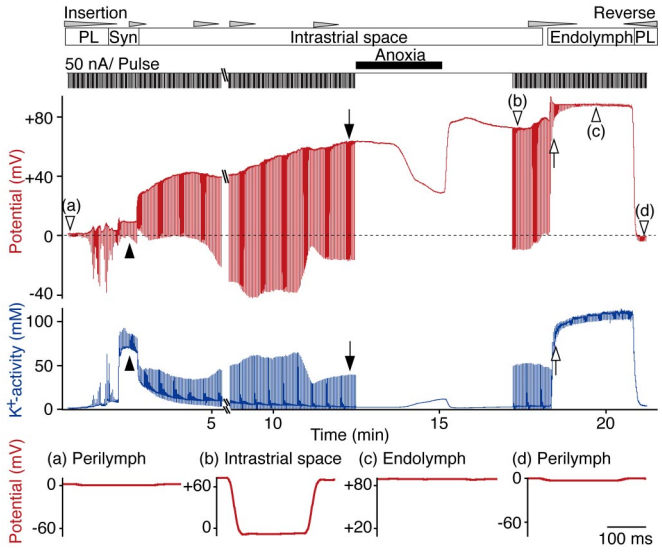

Fig. 3. The input resistance of lateral-wall compartments. A double-barreled K^+-selective electrode was driven through the lateral wall to record the potential (red) and aK^+ (blue); the input resistance was measured simultaneously as downward deflections in response to current pulses (50-nA/pulse, duration 200 msec) in the potential record. The upward deflections in the recording of aK^+ are artifacts resulting from the current pulses applied to the neighboring potential electrode. The electrode encountered successively the perilymph (PL), the syncytium (Syn, filled arrowheads), the IS (filled arrows), and finally the endolymph (EL) (open arrows). Note the decline in the ISP during a period of anoxia (see Fig. 4). Expanded traces of the voltage responses to individual current pulses (open arrowheads, *a*–*d*) are shown below the main traces.

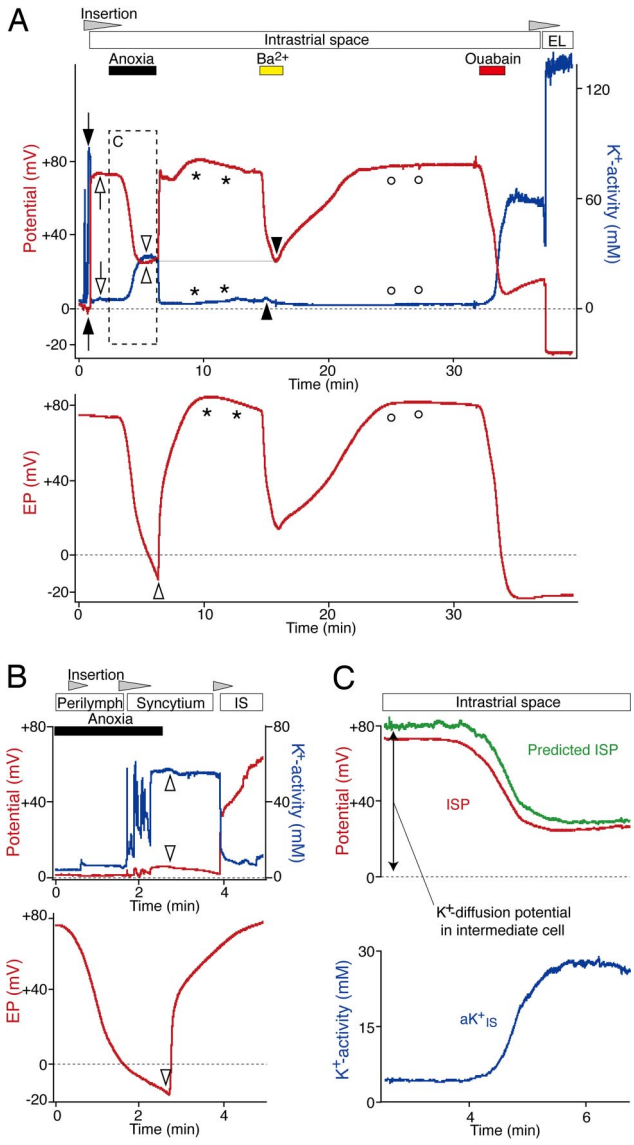

Fig. 4. Effects of blocking Na^+,K^+-ATPase and K^+ channels. (*A*) After passing through the syncytium (filled arrows), a K^+-selective electrode (*Upper*) was held in the IS (open arrows). The EP in a distinct portion of the cochlear turn was monitored simultaneously with a single-barreled electrode (*Lower*). Open and filled arrowheads show the peak changes in the potentials (red) and aK^+ (blue) during anoxia and vascular perfusion of Ba^{2+} (1 mM). Anoxia increased aK^+_{IS} much more than did the application of Ba^{2+}, but both treatments reduced the ISP to a similar value (thin horizontal line). The asterisks and open circles mark the overshoots of the potential and aK^+. After Ba^{2+} was washed out, ouabain (1 mM) was perfused. The K^+-selective electrode was finally inserted into the EL. (*B*) During a period of anoxia, the K^+-selective electrode (*Upper*) was advanced through the lateral wall and held in the syncytium. Even though the EP monitored by an electrode in the endolymph reached a negative value (*Lower*, open arrowhead), the K^+-selective electrode encountered negligible changes in the potential and aK^+ compared with normoxic conditions (see SI Fig. 7). When the animal was released from anoxia, little change was detected in aK^+ and potential in the syncytium (*Upper*, open arrowheads). When the electrode was advanced into the IS, it recorded the recovery of the ISP from anoxia. (*C*) The ISP during anoxia was predicted (green) with the equation, $ISP = V_{Syn} + (RT/F)\ln(aK^+_{i(Syn)}/aK^+_{IS})$. The potential and aK^+ in the syncytium (V_{Syn} and $aK^+_{i(Syn)}$) and aK^+_{IS} (blue) were obtained from *A* (*Upper*, filled arrowheads and box). The ISP recorded in *A* is also shown (red).

systems. Each blocker was perfused into the left vertebral artery, from which capillaries extend into the stria vascularis (20, 21).

We inhibited Na^+,K^+-ATPase by anoxia or ouabain and Kir4.1 channels by Ba^{2+}. During anoxia, aK^+_{IS} increased from 4 to 28 mM and then slightly decreased by 2 mM, whereas the ISP declined from +70 to +22 mV before rising by 3 mV (Fig. 4*A*; see also Fig. 4*C*). However, the EP declined monotonically to −14 mV. The responses of the ISP and aK^+_{IS} were therefore biphasic, whereas that of the EP was monophasic. Upon reoxygenation, the EP, ISP, and aK^+_{IS} gradually recovered and exhibited slight overshoots before returning to their initial values. We observed similar results in seven other experiments.

Ouabain (1 mM), a specific blocker of Na^+,K^+-ATPase, had effects similar to those of anoxia on the EP, ISP, and aK^+_{IS} in three experiments (Fig. 4*A*). The difference between the responses of ISP and EP was again clear: even during the slight rebound phase of the ISP and aK^+_{IS}, the EP continued to decline and reached a plateau of −22 mV (Fig. 4*A*). This difference was confirmed when the double-barreled electrode was advanced into the endolymph and recorded essentially the same potential as another electrode in the endolymph (Fig. 4*A*). Perfusion of the NKCC blocker bumetanide (1 mM) altered the EP, ISP, and aK^+_{IS} in a manner similar to anoxia and ouabain (SI Fig. 8). We also measured the ISP and aK^+_{IS} during vascular perfusion of Ba^{2+} (1 mM), which suppresses the EP (20, 21). Although the ISP declined from +71 to +23 mV, aK^+_{IS} rose by only 2.0 mM (Fig. 4*A*). This slight elevation of aK^+_{IS} might result from the blockage of Na^+,K^+-ATPase by ischemia because of the contraction of smooth muscle cells in some vessels between the vertebral artery and the strial capillaries, which could be caused by inhibition of their K^+ channels with Ba^{2+}, as reported in various arteries (30). Upon removal of Ba^{2+}, the ISP and aK^+_{IS} recovered and exhibited slight overshoots. Similar results were obtained in two additional trials. These data imply that the Ba^{2+}-sensitive channel Kir4.1 is critically involved in the generation of the ISP (19, 28).

The potential and intracellular aK^+ of the syncytium [V_{Syn} and

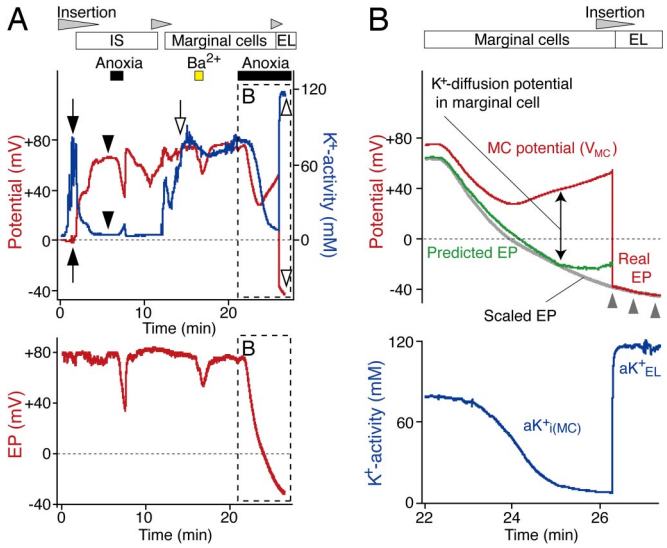

Fig. 5. Identification of MCs and analysis of their properties. (*A*) A K^+-selective electrode (*Upper*) advanced from the perilymph first encountered the syncytium (filled arrows) and the IS (filled arrowheads) toward the endolymph. Anoxia was imposed briefly when the electrode was in the IS. Entry into the MCs was signaled by a highly positive potential and elevated aK^+ (open arrow). Ba^{2+} (1 mM) and anoxia were tested while the electrode was held at that location. The electrode was ultimately inserted into the endolymph during a period of anoxia (open arrowheads). Throughout the experiment, the EP was recorded with a second electrode (*Lower*). (*B*) The EP during anoxia was predicted (green) with the equation, $EP = V_{MC} + (RT/F)\ln(aK^+_{i(MC)}/aK^+_{EL})$. The potential ($V_{MC}$, red) and intracellular aK^+ ($aK^+_{i(MC)}$, blue) of MCs and the endolymphatic aK^+ (aK^+_{EL}) were obtained from *A* (*Upper*, box and open arrowhead). The vertical scale of the EP in *A* (*Lower*, box) was adjusted (scaled EP, gray line) to fit the curve of the potential that was recorded by the K^+-selective electrode when it was in endolymph (red line highlighted by gray arrowheads).

$aK^+_{i(Syn)}$] are expected to be stable. Indeed, we found in two experiments that these values barely altered even when the EP reached a negative value during anoxia (Fig. 4*B*). The ISP may therefore be calculated as the sum of V_{Syn} and the potential difference across the apical membranes of ICs,

$$ISP = V_{Syn} + \frac{RT}{F}\ln\left(\frac{P_K{\cdot}aK^+_{i(Syn)} + P_{Na}{\cdot}aNa^+_{i(Syn)} + P_{Cl}{\cdot}aCl^-_{IS}}{P_K{\cdot}aK^+_{IS} + P_{Na}{\cdot}aNa^+_{IS} + P_{Cl}{\cdot}aCl^-_{i(Syn)}}\right),$$

where $aK^+_{i(Syn)}$, $aNa^+_{i(Syn)}$, and $aCl^-_{i(Syn)}$ are the intracellular ionic activities of the syncytium; aK^+_{IS}, aNa^+_{IS}, and aCl^-_{IS} are the ionic activities in the IS fluid; P_K, P_{Na}, and P_{Cl} are the permeability coefficients for the ions; and R, T, and F have their usual meanings.

An earlier patch–clamp analysis revealed that K^+ conductance dominated the apical membranes of isolated ICs (31), implying that P_K greatly exceeds P_{Na} and P_{Cl}. We therefore calculated the ISP during anoxia with the assumption that it represents the sum of V_{Syn} and the K^+ equilibrium potential (E_K) across the apical membranes of ICs. The predicted ISP closely corresponded to the measured potential, although the former was slightly more positive (Fig. 4*C*). Because the membrane potential of isolated ICs is slightly more positive than E_K (32), the difference may reflect a small contribution of Na^+ or Cl^- conductance in the apical membranes of ICs. We observed similar results in two additional experiments. It is therefore likely that the ISP is generated primarily by Ba^{2+}-sensitive K^+ diffusion across the apical membranes of ICs whereas the low $[K^+]_{IS}$ is maintained by Na^+,K^+-ATPase and NKCC.

The Involvement of MCs in Formation of the EP. Because the only component between the IS and the endolymphatic space is a monolayer of MCs, these cells must be responsible for the different behaviors of the EP and ISP during anoxia or perfusion of blockers. We therefore examined the electrochemical qualities of the MCs. After encountering compartments exhibiting the features of the syncytium and the IS during the insertion of a K^+-selective electrode, we detected a highly positive potential similar to the ISP and an increase of aK^+ to 77 mM (Fig. 5*A*). Because this aK^+ value was as high as that in the syncytium (79 mM, Fig. 5*A*) but lower than that in the endolymph (>100 mM; see Figs. 3 and 4), we surmised this compartment represented the cytoplasm of the MCs.

The arterial perfusion of Ba^{2+} during recordings at this position reduced the potential by 20 mV but caused little change of aK^+ (Fig. 5*A*); similar results were obtained in two trials. After washing out Ba^{2+}, we applied anoxia. Whereas aK^+ declined in a sigmoidal fashion and finally reached a plateau at 8 mM, the potential declined from +74 mV to +27 mV and then rebounded to +52 mV. Similar results were recorded in two experiments. This potential alteration resembled that of the ISP (see Fig. 4*A*) but did not correlate with that of EP monitored with a separate electrode (Fig. 5*A*). The changes were reversible after reoxygenation in five experiments (SI Fig. 9*A*). When the K^+-selective electrode was advanced into the endolymph during anoxia, it recorded a potential of −41 mV and aK^+ of 116 mM (Fig. 5*A*). This result strongly suggests that a large potential difference occurred across the apical membranes of the MCs.

The basolateral membranes of MCs express little K^+ conductance (33), whereas their apical surfaces facing the endolymph bear the K^+ channel KCNQ1/KCNE1 (23–25). If these channels provide another pathway for K^+, a reduction of aK^+ in the MCs should accelerate the diffusion of K^+ from the endolymph into the MCs and enlarge the potential difference across their apical membranes. To test this idea, we compared the recorded EP with that calculated from the MC potential (V_{MC}) and potential difference across the apical membrane of MCs by the relation

$$EP = V_{MC} + \frac{RT}{F}\ln\left(\frac{P_K{\cdot}aK^+_{i(MC)} + P_{Na}{\cdot}aNa^+_{i(MC)} + P_{Cl}{\cdot}aCl^-_{EL}}{P_K{\cdot}aK^+_{EL} + P_{Na}{\cdot}aNa^+_{EL} + P_{Cl}{\cdot}aCl^-_{i(MC)}}\right),$$

where $aK^+_{i(MC)}$, $aNa^+_{i(MC)}$, $aCl^-_{i(MC)}$, aK^+_{EL}, aNa^+_{EL}, and aCl^+_{EL} are ionic activities of the inside of MCs and endolymph. Because anoxia reduced the EP with little change of aK^+_{EL} (SI Fig. 9*A*) (34), aK^+_{EL} is constant. It was reported that the K^+ permeability is considerably larger than the Na^+ and Cl^- permeabilities in the apical membranes of MCs (35–37). We presumed that K^+ permeability dominated the apical membrane of MCs and simply calculated the EP as the sum of V_{MC} and the E_K of MCs during anoxia (Fig. 5*B*). The measured EP was scaled to fit the trace recorded by the K^+-selective electrode when it was in endolymph (Fig. 5*B*). The predicted and scaled EPs matched well, although the former was slightly more positive than the latter. This finding suggests that the potential difference across the apical membranes of MCs can be attributed largely to the K^+-selective diffusion potential. The subtle difference between the estimated and recorded traces (Fig. 5*B*) may be caused by other conductances than that to K^+. Finally, we found that vascular perfusion of ouabain and bumetanide reduced the MC potential and $aK^+_{i(MC)}$ in a manner similar to anoxia (SI Fig. 9 *B* and *C*).

Discussion

We have confirmed the existence of the IS and its unique electrochemical properties (Figs. 2 and 3). Moreover, we have shown that blockage of K^+ transporters (NKCC and Na^+,K^+-ATPase) or of K^+ channel Kir4.1 suppresses the ISP and EP by

distinct mechanisms, respectively through an increase of aK^+_{IS} or direct inhibition of K^+ diffusion (Fig. 4*A*). The recorded alternation of the ISP corresponded with the estimated change of E_K on the apical membranes of ICs (Fig. 4*C*). These results not only verify that the EP originates from the ISP but also indicate that the potential difference across the membranes of ICs can be explained largely as a K^+ diffusion potential and underlies the ISP (26, 28).

We identified three other factors crucial for the formation of the EP. First, the IS exhibits a high input resistance (Fig. 3), indicating that this space is electrically isolated from the neighboring fluids. This feature is required for sustaining the highly positive ISP. The layers of BCs, MCs, and vascular endothelia that separate the IS from, respectively, the perilymph, endolymph, and blood with tight junctions must act as insulators. Consistent with this argument, knockout of claudin-11 and connexin30, which disrupt the tight junctions of, respectively, BCs and endothelia, cause a large reduction in the EP (9, 38–40). Arterially perfused reagents such as Ba^{2+}, ouabain, and bumetanide can nonetheless penetrate the strial endothelium and reach the IS to produce their effects on the EP. The endothelial barrier may therefore be loose enough to permit the diffusion of these molecules and yet tight enough to guarantee the high-input resistance of the IS. The prominently infolded membranes of ICs and MCs tightly wrap the capillaries, and the space between them is narrow (8). These anatomical features may provide a mechanism of increasing the resistance between the IS and blood while permitting the diffusion of reagents from the blood to the IS.

A second consideration is that the syncytium is virtually clamped at 0 ≈+4 mV (Figs. 2 and 4*B*, see also SI Fig. 7). Gap junctions interconnect many fibrocytes, thereby establishing a large cellular volume associated with a high membrane capacitance. Even if the magnitude of K^+ transport through the lateral wall should alter, the potential of syncytium would barely change. Because of this, the K^+-diffusion potential at the apical membranes of ICs can form a significant fraction of the ISP.

The third feature is K^+ diffusion across the apical membranes of MCs. When the basolateral Na^+,K^+-ATPase in MCs is inhibited, the predicted change in E_K at the apical membrane of ICs nearly equaled the reduction of the ISP but not that of the EP (Fig. 4). This difference could be attributed to the KCNQ1/KCNE1-mediated K^+-diffusion potential across the apical membrane of MCs, which would be enlarged by the reduction of $aK^+_{i(MC)}$ (Fig. 5). This reduction could be caused by K^+ efflux from MCs into endolymph, for the membrane potential of MCs relative to EP consistently exceeds E_K (Fig. 5*B*).

We propose that the EP comprises two different K^+-diffusion potentials, one across the apical membrane of the ICs and the other across the apical side of the MCs:

$$EP = V_{Syn} + \frac{RT}{F}\ln\left(\frac{aK^+_{i(Syn)}}{aK^+_{IS}}\right) + \frac{RT}{F}\ln\left(\frac{aK^+_{i(MC)}}{aK^+_{EL}}\right).$$

The electrochemical properties of the lateral wall in the normal conditions and during the blockage of the K^+-transport mechanisms in the strial vascularis are summarized in Fig. 6. Under physiological conditions, aK^+_{EL} moderately exceeds $aK^+_{i(MC)}$ (Fig. 5*A* and SI Fig. 9*A*), so the difference of 10 mV between the EP and the MC potential (29, 41) is likely to be generated by K^+ diffusion. The negative EP that is induced by strong block of strial K^+ transporters results from the combination of a decrease in the ISP and an increase in the potential difference across the MCs' apical membranes (Figs. 4 and 5), rather than from elements in the organ of Corti (42).

Although the H^+,K^+-ATPase expressed in the basolateral membranes of MCs may also participate in EP formation (43), its involvement and the dynamics of strial pH in regulation of the

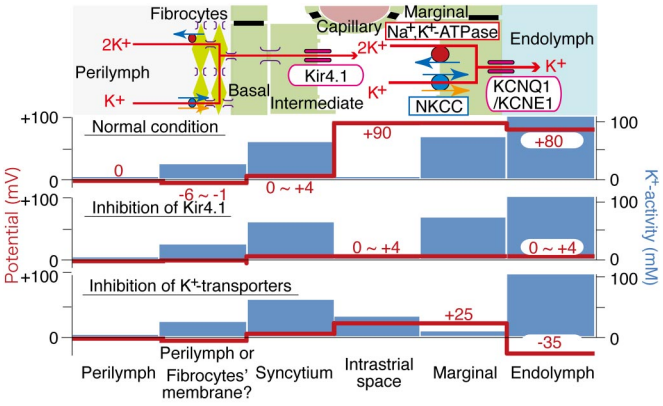

Fig. 6. Summary profile of electrochemical properties of the lateral cochlear wall. *Upper* depicts the structure of the lateral wall and the K^+-transport apparatus involved in the generation of the EP. The predicted potential and aK^+ in each compartment under normal condition and inhibition of Kir4.1 and the strial K^+-transporters are respectively shown in other images. The moderately elevated aK^+ of 20 mM in the second compartment from the left may result from the electrode's occasionally penetrating the convoluted membranes of fibrocytes.

electrochemical milieu of the IS remain elusive. Because Na^+,K^+-ATPase and NKCC coexist in the basolateral membranes of MCs, Na^+ is expected to cycle between these two transporters (Fig. 1*B*). This cycling seems to couple the Na^+ efflux through Na^+,K^+-ATPase and the influx through NKCC, which would be required for K^+ uptake from the IS to MCs. K^+ taken up by the cycling mechanism may also exit from the MCs' apical KCNQ1/KCNE channels into the endolymph. In support of this idea, inhibition of either transporter completely suppresses the EP (14). The cycling of Na^+ across the basolateral membrane may therefore play an essential role in unidirectional K^+ transport from the IS to endolymph through MCs. This K^+ dynamics would also be important in maintaining the high $[K^+]$ in endolymph.

Materials and Methods

Information regarding the preparation of double-barreled K^+-selective electrodes, vascular perfusion, and measurement of potential, aK^+, and input resistance in the cochlear lateral wall is provided in *SI Text*.

Animal Preparation and Solutions. The experimental protocol was approved by the Animal Research Committee of Osaka University Medical School. The experiments were carried out under the supervision of the Committee and in accordance with the Guidelines for Animal Experiments of Osaka University and the Japanese Animal Protection and Management Law. The guinea pigs were fed and allowed free access to water.

Albino guinea pigs (200–250 g) were deeply anesthetized intramuscularly with pentobarbital sodium (30 mg/kg; Nembutal, Abbott), paralyzed by i.v. injection of pancuronium bromide (3 mg/kg), and artificially respirated. For vascular perfusion, ouabain and barium chloride were dissolved in control solution containing 136.5 mM NaCl, 5.4 mM KCl, 1.8 mM $CaCl_2$, 0.53 mM $MgCl_2$, 5.5 mM glucose, and 5.0 mM Hepes at pH 7.4. Bumetanide was dissolved before use in control solution with 1% ethanol, a solution without effect on the EP.

ACKNOWLEDGMENTS. We thank Drs. A. James Hudspeth (The Rockefeller University) and I. Findlay (Université de Tours, Tours, France) for their critical reading of this manuscript and Dr. N. Abe for technical comments. This work was supported by the following research grants: Leading Project for Biosimulation "Development of Models for Disease and Drug Action" (to Y.K.), Grant-in-Aid for Scientific Research on Priority Areas 17081012 (to H.H.), Grant-in-Aid for Young Scientists (B) 19790188 (to H.H.), the Global COE Program "*in silico* medicine" at Osaka University (to F.N., H.H., and Y.K.), and a grant for "Research and Development of Next-Generation Integrated Life Simulation Software" (to Y.K.), from the Ministry of Education, Culture, Sport, Science and Technology of Japan, and Takeda Science Foundation (to H.H.).

1. von Békésy G (1952) DC resting potentials inside the cochlear partition. *J Acoust Soc Am* 24:72–76.
2. Hudspeth AJ (1989) How the ear's works work. *Nature* 341:397–404.
3. Hibino H, Kurachi Y (2006) Molecular and physiological bases of K^+ circulation in the mammalian inner ear. *Physiology (Bethesda)* 21:336–345.
4. Chan DK, Hudspeth AJ (2005) Ca^{2+} current-driven nonlinear amplification by the mammalian cochlea *in vitro*. *Nat Neurosci* 8:149–155.
5. Kikuchi T, Adams JC, Miyabe Y, So E, Kobayashi T (2000) Potassium ion recycling pathway via gap junction systems in the mammalian cochlea and its interruption in hereditary nonsyndromic deafness. *Med Electron Microsc* 33:51–56.
6. Wangemann P (2002) K^+ cycling and the endocochlear potential. *Hear Res* 165:1–9.
7. Spicer SS, Schulte BA (1998) Evidence for a medial K^+ recycling pathway from inner hair cells. *Hear Res* 118:1–12.
8. Hinojosa R, Rodriguez-Echandia EL (1966) The fine structure of the stria vascularis of the cat inner ear. *Am J Anat* 118:631–663.
9. Cohen-Salmon M, Regnault B, Cayet N, Caille D, Demuth K, Hardelin JP, Janel N, Meda P, Petit C (2007) Connexin30 deficiency causes instrastrial fluid-blood barrier disruption within the cochlear stria vascularis. *Proc Natl Acad Sci USA* 104:6229–6234.
10. Takeuchi S, Ando M (1998) Dye-coupling of melanocytes with endothelial cells and pericytes in the cochlea of gerbils. *Cell Tissue Res* 293:271–275.
11. Jahnke K (1975) The fine structure of freeze-fractured intercellular junctions in the guinea pig inner ear. *Acta Otolaryngol Suppl* 336:1–40.
12. Nakazawa K, Spicer SS, Schulte BA (1995) Ultrastructural localization of Na,K-ATPase in the gerbil cochlea. *J Histochem Cytochem* 43:981–991.
13. Crouch JJ, Sakaguchi N, Lytle C, Schulte BA (1997) Immunohistochemical localization of the Na-K-Cl cotransporter (NKCC1) in the gerbil inner ear. *J Histochem Cytochem* 45:773–778.
14. Kusakari J, Ise I, Comegys TH, Thalmann I, Thalmann R (1978) Effect of ethacrynic acid, furosemide, and ouabain on the endollymphatic potential and upon high energy phosphates of the stria vascularis. *Laryngoscope* 88:12–37.
15. Dixon MJ, *et al*. (1999) Mutation of the Na-K-Cl cotransporter gene Slc12a2 results in deafness in mice. *Hum Mol Genet* 8:1579–1584.
16. Delpire E, Lu J, England R, Dull C, Thorne T (1999) Deafness and imbalance associated with inactivation of the secretory Na-K-2Cl cotransporter. *Nat Genet* 22:192–195.
17. Flagella M, *et al*. (1999) Mice lacking the basolateral Na-K-2Cl cotransporter have impaired epithelial chloride secretion and are profoundly deaf. *J Biol Chem* 274:26946–26955.
18. Ando M, Takeuchi S (1999) Immunological identification of an inward rectifier K^+ channel (Kir4.1) in the intermediate cell (melanocyte) of the cochlear stria vascularis of gerbils and rats. *Cell Tissue Res* 298:179–183.
19. Hibino H, *et al*. (2004) Expression of an inwardly rectifying K^+ channel, Kir5.1, in specific types of fibrocytes in the cochlear lateral wall suggests its functional importance in the establishment of endocochlear potential. *Eur J Neurosci* 19:76–84.
20. Marcus DC, Rokugo M, Thalmann R (1985) Effects of barium and ion substitutions in artificial blood on endocochlear potential. *Hear Res* 17:79–86.
21. Hibino H, *et al*. (1997) An ATP-dependent inwardly rectifying potassium channel, K_{AB}-2 (Kir4.1), in cochlear stria vascularis of inner ear: its specific subcellular localization and correlation with the formation of endocochlear potential. *J Neurosci* 17:4711–4721.
22. Marcus DC, Wu T, Wangemann P, Kofuji P (2002) KCNJ10 (Kir4.1) potassium channel knockout abolishes endocochlear potential. *Am J Physiol* 282:C403–C407.
23. Sakagami M, *et al*. (1991) Cellular localization of rat Isk protein in the stria vascularis by immunohistochemical observation. *Hear Res* 56:168–172.
24. Vetter DE, *et al*. (1996) Inner ear defects induced by null mutation of the Isk gene. *Neuron* 17:1251–1264.
25. Casimiro MC, *et al*. (2001) Targeted disruption of the Kcnq1 gene produces a mouse model of Jervell and Lange-Nielsen Syndrome. *Proc Natl Acad Sci USA* 98:2526–2531.
26. Salt AN, Melichar I, Thalmann R (1987) Mechanisms of endocochlear potential generation by stria vascularis. *Laryngoscope* 97:984–991.
27. Ikeda K, Morizono T (1989) Electrochemical profiles for monovalent ions in the stria vascularis: cellular model of ion transport mechanisms. *Hear Res* 39:279–286.
28. Takeuchi S, Ando M, Kakigi A (2000) Mechanism generating endocochlear potential: role played by intermediate cells in stria vascularis. *Biophys J* 79:2572–2582.
29. Melichar I, Syka J (1987) Electrophysiological measurements of the stria vascularis potentials in vivo. *Hear Res* 25:35–43.
30. Jackson WF (2005) Potassium channels in the peripheral microcirculation. *Microcirculation* 12:113–127.
31. Takeuchi S, Ando M (1998) Inwardly rectifying K^+ currents in intermediate cells in the cochlea of gerbils: a possible contribution to the endocochlear potential. *Neurosci Lett* 247:175–178.
32. Takeuchi S, Ando M (1999) Voltage-dependent outward K^+ current in intermediate cell of stria vascularis of gerbil cochlea. *Am J Physiol* 277:C91–C99.
33. Takeuchi S, *et al*. (1995) Ion channels in basolateral membrane of marginal cells dissociated from gerbil stria vascularis. *Hear Res* 83:89–100.
34. Melichar I, Syka J (1977) Time course of anoxia-induced K^+ concentration changes in the cochlea measured with K^+ specific microelectrodes. *Pflügers Arch* 372:207–213.
35. Takeuchi S, Marcus DC, Wangemann P (1992) Ca^{2+}-activated nonselective cation, maxi K^+ and Cl^- channels in apical membrane of marginal cells of stria vascularis. *Hear Res* 61:86–96.
36. Wangemann P, Liu J, Marcus DC (1995) Comparison of ion transport mechanisms between vestibular dark cells and strial marginal cells. *Hear Res* 84:19–29.
37. Shen Z, Marcus DC (1998) Divalent cations inhibit IsK/KvLQT1 channels in excised membrane patches of strial marginal cells. *Hear Res* 123:157–167.
38. Kitajiri S, *et al*. (2004) Compartmentalization established by claudin-11-based tight junctions in stria vascularis is required for hearing through generation of endocochlear potential. *J Cell Sci* 117:5087–5096.
39. Gow A, *et al*. (2004) Deafness in Claudin 11-null mice reveals the critical contribution of basal cell tight junctions to stria vascularis function. *J Neurosci* 24:7051–7062.
40. Teubner B, *et al*. (2003) Connexin30 (Gjb6)-deficiency causes severe hearing impairment and lack of endocochlear potential. *Hum Mol Genet* 12:13–21.
41. Offner FF, Dallos P, Cheatham MA (1987) Positive endocochlear potential: mechanism of production by marginal cells of stria vascularis. *Hear Res* 29:117–124.
42. Kusakari J, *et al*. (1983) Generation mechanism of the negative endocochlear potential during early stage of anoxia. *ORL J Otorhinolaryngol Relat Spec* 45:195–202.
43. Shibata T, *et al*. (2006) Gastric type H^+,K^+-ATPase in the cochlear lateral wall is critically involved in formation of the endocochlear potential. *Am J Physiol* 291:C1038–C1048.